Applied Thermal Engineering 116 (2017) 292–302

Contents lists available at ScienceDirect

Applied Thermal Engineering

journal homepage: www.elsevier.com/locate/apthermeng

Research Paper

Simulation of a multi-source hybrid heat pump system with seasonal thermal storage in cold regions

Zongwei Han *, Lejian Qu, Xiao Ma, Xiaobei Song, Changming Ma

SEP Key Laboratory of Eco-Industry, School of Metallurgy, Northeastern University, Shenyang 110819, PR China

HIGHLIGHTS

- A novel multi-source hybrid heat pump system with seasonal thermal storage is constructed.
- Mathematical model of the heating and air conditioning system was established.
- The performance of the multi-source hybrid heat pump system and ground source heat pump system is simulated and compared.
- The applicability of the multi-source hybrid heat pump system in different climate regions is investigated.

ARTICLE INFO

Article history:
Received 24 October 2016
Revised 28 December 2016
Accepted 15 January 2017
Available online 18 January 2017

Keywords:
Cold regions
Multi-source hybrid heat pump
Simulation analysis
Energy-saving rate
Soil thermal balance

ABSTRACT

Based on taking full account of the building load and renewable energy output characteristics in cold regions, a multi-source hybrid heat pump system (MSHHPS) with seasonal thermal storage was proposed. The seasonal thermal storage comprehensively utilized solar energy, geothermal energy and air energy. The composition and operation modes of the system were introduced. The mathematical model of the main parts of the proposed system was established. The transition condition of the different operating modes of the system was determined. Taking a building in Harbin as the object for simulation analysis, the operation effect and the change of the soil temperature field of the system were obtained. The results showed that: The average coefficient of performance (*COP*) of the MSHHPS with seasonal thermal storage was 3.06 (in the Harbin region for 10 years), the soil thermal balance rate was 100.33% and the energy-saving rate was 29.84% comparing to the ground source heat pump system (GSHPS). For the initial investment, MSHHPS only required additional double-source heat pump unit, which accounted at 9.59%. The static payback period of the double-source heat pump unit was 4 years. The system can maintain efficient and economical operation in the typical cold regions.

1. Introduction

The energy consumption of buildings, which relies a lot of electricity and fossil fuels, constitutes heavily to the total world energy consumption. The International Energy Agency (IEA) pointed out that the energy consumption of buildings accounted for about 35% of the total world energy consumption, while some developed countries (the United States, Japan, Germany, Britain, etc.) had even reached 40% of the total world energy consumption [1]. In the cold regions, the heating and air conditioning account for the largest proportion of building energy consumption, as it requires prolong heating period and covers a large area. There is a need to prioritize the reduction in emission and ultimately contribute to building savings.

Heat pump technology can convert low-grade energy (air, soil, solar, industrial waste, etc.) to "environmental friendly" high-grade energy. It can reduce fuel combustion pollution of the environment and bring global environmental benefits. In the cold regions, there are some operational issues with single-source heat pump systems: (1) When the outdoor temperature is low, the outdoor heat exchanger frosts, the performance and operation reliability of the system decreases [2–4]; (2) In cold regions, the soil thermal imbalance problem can be caused by continuous running of ground-source heat pump system (GSHPS) with uneven heating and cooling loads. Hence, the performance and reliability of the GSHPS decreases gradually [5–9]; (3) Due to the low density of solar heat flux, its characteristics are intermittent and unstable. Hence, the application of solar heat pumps in cold regions will require a large collector area, which will lead to a high initial investment and installation difficulties [10–12].

* Corresponding author.
E-mail address: hanzongwei_neu@163.com (Z. Han).

http://dx.doi.org/10.1016/j.applthermaleng.2017.01.057
1359-4311/

Nomenclature

A_i	the pipe inner surface area of heat exchanger (m^2)
A_o	the pipe outer surface area of the heat exchanger (m^2)
A_3	the pipe outer surface area of the collector/evaporator (m^2)
A'_3	the collector/evaporator surface's total solar radiation receiving area (m^2)
A_v	the sectional area of the valve (m^2)
COP	annual average coefficient of performance
COP_c	the average heating coefficient of performance
COP_h	the average cooling coefficient of performance
COP_x	coefficient of performance of separated type heat pipe soil heat storage mode
D_{eq}	equivalent diameter of buried pipe (m)
F	the barrier factor
G_{room}	the indoor heat capacity (W)
GSHPS	ground source heat pump system
H	the height of the fin (m)
I	the solar irradiation per unit area (W/m^2)
IEA	International Energy Agency
L	the length of the fin (m)
M_{com}	refrigerant quantities in compressor (kg)
M_{sp}	refrigerant quantities of the single-phase regions (kg)
M_{tp}	refrigerant quantities of the two-phase regions (kg)
MSHHPS	multi-source hybrid heat pump system
N_u	the refrigerant Nusselt number
P	the system power consumption (J)
P_{hp}	heat pump units power consumption (J)
P_r	the refrigerant Prandtl number
Q_{as}	heat transfer capacity of the air side (J)
Q_c	cold supply (J)
Q_h	heat supply (J)
Q_{hp}	heating capacity of heat pump unit (J)
Q_l	the power of dissipation (J)
Q_w	heat transfer of the refrigerant side (J)
S	the fin spacing (m)
T_{am}	the average temperature of the air (°C)
T_{bf}	annual surface temperature fluctuations (°C)
T_{co}	outlet water temperature of condenser (°C)
T_{ci}	inlet water temperature of condenser (°C)
T_{ei}	inlet fluid temperature of evaporator (°C)
T_{eo}	outlet water temperature of evaporator (°C)
T_{odl}	mode 4 close temperature (°C)
T_{rm}	average temperature of refrigerant (°C)
T_{rcd}	indoor design temperature in the cooling period (°C)
T_{rhd}	indoor design temperature in the heating period (°C)
TRNSYS	Transient System Simulation Program
T_s	soil temperature (°C)
T_{sc}	mode 2 temperature control parameter (°C)
T_{sf}	heat transfer fluid temperature within the soil heat exchanger (°C)
T_{sm}	the annual average temperature of ground surface (°C)
T_{so}	undisturbed soil temperature (°C)
T_{srl}	nodal temperatures of the first layer of soil (°C)
T_{tw}	temperature of the pipe wall (°C)
T_w	cooling water average temperature (°C)
T_z	ambient temperature (°C)
ΔT	temperature difference of air-side (°C)
V_h	the theoretical displacement (m^3)
X	distance from a point at the fin end cut through the rays of the sun to the incident point after the fin (m)
Y	distance from the incident point to the plane coil (m)
α	the solar azimuth (°)
α_{ai}	air-side convection heat transfer coefficient of the collector/evaporator [$W/(m^2 \cdot °C)$]
α_{aj}	radiation heat transfer coefficient of the collector/evaporator [$W/(m^2 \cdot °C)$]
α_{as}	convection heat transfer coefficient of the collector/evaporator [$W/(m^2 \cdot °C)$]
α_c	convection heat transfer coefficient of the condenser [$W/(m^2 \cdot °C)$]
α_{il}	convection heat transfer coefficient of refrigerant [$W/(m^2 \cdot °C)$]
α'_{il}	heat transfer coefficient of refrigerant in single-phase zone [$W/(m^2 \cdot °C)$]
α''_{il}	heat transfer coefficient of refrigerant in single-phase zone [$W/(m^2 \cdot °C)$]
a_w	heat transfer coefficient of the cooling water [$W/(m^2 \cdot °C)$]
a_s	thermal conductivity of soil (m^2/s)
c	calculating coefficient
c_{ps}	specific heat of soil [$J/(kg \cdot °C)$]
c_{psf}	specific heat of exchange fluid [$J/(kg \cdot °C)$]
c_{vf}	expansion valve flow coefficient[$J/(kg \cdot °C)$]
d_i	internal diameter of pipe (m)
d_o	external diameter of pipe (m)
d_t	allowed indoor temperature fluctuation(°C)
d_{to}	mode 1 start temperature difference (°C)
h_{r1}, h_{r2}	import and export enthalpy of refrigerant of the condenser (kJ/kg)
h_{r3}, h_{r4}	import and export enthalpy of refrigerant of the collector/evaporator (kJ/kg)
h_{v1}, h_{v2}	the specific enthalpy values before and after the throttle (kJ/kg)
h_{w1}, h_{w2}	import and export enthalpy of the cooling water (kJ/kg)
h	the solar elevation angle (°)
h_a	convection heat transfer coefficient of the surface air [$W/(m^2 \cdot °C)$]
h_{sf}	convection heat transfer coefficient of heat transfer fluid [$W/(m^2 \cdot °C)$]
l_o	length of borehole heat exchanger (m)
θ_T	the collector/evaporator angle (°)
φ	the radiation efficiency
m_r	the mass flow of refrigerant (kg/s)
m_w	the mass flow of cooling water (kg/s)
m_v	the volume flow of refrigerant (m^3/s)
p_c	condensation pressure (Pa)
p_e	evaporation pressure (Pa)
Δp_v	pressure drop between the inlet and outlet valves (Pa)
q_l	heat exchange capacity per unit length (W/m)
r	radial coordinate (m)
r_0	borehole heat exchangers' spacing (m)
t_0	time from initial time of simulation to eventual time of maximum temperature for ground surface (h)
t	time (h)
t_c	time constant (h)
v_{ci}	compressor's suction specific volume of refrigerant (m^3/kg)
v_{sf}	borehole heat exchangers' inlet velocity (m/s)
z	axial coordinate (m)
z_0	depth (m)
ρ_f	density of liquid refrigerant (kg/m^3)
ρ_g	density of gas refrigerant (kg/m^3)
ρ_{vi}	the inlet refrigerant density of expansion valve (kg/m^3)
ρ_s	density of soil (kg/m^3)

ρ_{sf}	density of heat transfer fluid (kg/m^3)	η_v	the volumetric efficiency
x	the dryness of the refrigerant	λ_s	thermal conductivity of soil [W/(m$^{2\cdot}$°C)]
Θ	the saving rate of the system	κ	adiabatic coefficient
ε	the rate of soil thermal balance	a_1, b_1, c_1, a_2, b_2, c_2	curve-fit coefficients
η_i	the indicated efficiency		

To solve these problems, some scholars have tried to take advantage of complementary natural energy. Currently, the scholars are mainly engaged in the research of the solar-ground composite source heat pump system and air-solar composite heat pump system. Liu [13] proposed a solar-air composite heat source heat pump system and conducted a comprehensive experimental study of this system in the standard enthalpy difference laboratory. Liang [14] proposed a new solar-assisted air-source heat pump system with flexible operational modes to improve the performance of the heating system. By optimising the full use of solar energy and air energy, the efficiency and reliability of the composite heat pump system were significantly improved. However, the solar energy and the environment air energy in cold regions have isotropic distribution. The ambient temperature is low under the condition of low solar radiation so that it difficult to meet the heating requirements. Bakirci [15] proposed a solar-ground source heat pump heating system to make full use of solar energy and shallow soil energy. The experimental results showed that in the heating period across all of the Turkish cold regions, the daytime solar thermal efficiency was 33–54%, with the average coefficient of performance (*COP*) at about 3, and the heating heat pump system's *COP* was about 2.7. Girard and Trillat-Berdal [16,17] proposed a system to improve the feasibility of the ground-source heat pump through a solar collector. Si [18] designed a novel solar-ground source heat pump system for an office building in Beijing for heating, cooling, and producing domestic hot water. However, the limitation is that solar energy density is low in the cold regions. If solar energy is solely used to solve the problem of the soil thermal imbalance of ground-source heat pumps in cold regions, it will require a larger collection area, installation space and higher costs, meantime this increases the operation difficulty and action ability. As of now, there is less research on air-ground composite source heat pump systems. Pardo [19] proposed a system of a ground-source heat pump and energy storage composite air-source heat pump, and the system unit was optimized. This configuration obtained the highest cooling mode performance factor, with electrical energy consumptions achieved at around 60% and 82% compared with the air-source heat pump and ground-source heat pump configurations, respectively.

Composite source heat pump system is a good way of heating and air conditioning in severe cold regions, but the existing researches have their own problems to some extent. Considering the matching relationship between building load and the energy output characteristics of renewable energy sources, an efficient multi-source hybrid heat pump system (MSHHPS) with a novel double-source heat pump unit is proposed. The MSHHPS can comprehensively utilize ambient air and solar energy for seasonal thermal storage by novel collector/evaporator in non-heating period, then directly heat coupled with GSHP unit in heating period. Through establishing a mathematical model to simulate the system's annual operating characteristics and inspect the applicability and energy efficiency in typical cold regions, it can provide a reference for the comprehensive application of the system in the cold area.

2. Construction and operation modes of MSHHPS

Considering buildings load and renewable energy output characteristics in cold regions, a MSHHPS is proposed. As shown in Fig. 1, the system mainly consists of ground-source heat pump units, double-source heat pump unit (it can run as a separate heat pipe mode and vapor compression heating mode), a ground heat exchanger, air-conditioning terminal units, circulation pump and piping accessories and other components.

The double-source heat pump unit consists of a collector/evaporator, condenser, compressor, throttle device, gas–liquid separator, etc. It can switch between the vapor compression heat pump cycle and the separate heat pipe mode. The intermediate quasi two-stage compression heat pump cycle is used to improve the low-temperature heating performance. In the separate type heat pipe mode, the refrigerant in the collector/evaporator can absorb thermal and gasify; then the gas through the rising pipe to the condenser condenses into liquid by gravity and returns to the evaporator, allowing natural circulation in the heat pipes to be achieved. Taking into account the needs of summer indoor cooling and soil heat storage, the heat exchanger is divided into two series, one for cooling and another for heat storage.

The MSHHPS can achieve three heating modes, two cooling modes, and one heat storage mode:

Mode 1 – The double-source heat pump unit is operated at separated type heat pipe condition for soil heat storage;
Mode 2 – The cooling series of the soil-buried tubes is operated for direct cooling;
Mode 3 – The GSHP unit is operated for cooling;
Mode 4 – The double-source heat pump unit is operated at vapor compression condition for heating;
Mode 5 – The GSHP unit is operated for heating;
Mode 6 – The double-source heat pump unit (vapor compression condition) and GSHP unit are operated for combined heating.

3. Mathematical model

At present, there are many transient system simulation software, such as Transient System Simulation Program (TRNSYS). The collector/evaporator of double-source heat pump unit is significantly different in structure from the traditional evaporator. Furthermore, the double-source heat pump unit combine the vapor compression heat pump cycle and the separate heat pipe cycle. There is also a significant difference from the traditional vapor compression type. Therefore, the mathematical model is established to analyze the performance of MSHHPS.

3.1. Collector/evaporator

In order to make full use of the environmental air energy and solar energy, a collector/evaporator is applied to the heat pump cycle of heating in the heating period and to the separated type heat pipe soil heat storage mode in the non-heating period. The structure of collector/evaporator is similar with the ordinary air-cooled evaporator, taking single row serpentine coil form with rectangular fins, coated with selective absorbing coating in the heat exchanger pipes and fins. The heat exchange tubes and fins are made of copper tube and aluminum fin respectively. To reduce the flow resistance, the refrigerant is divided into pluralities of branches enter or go out the collector/evaporator. Because the

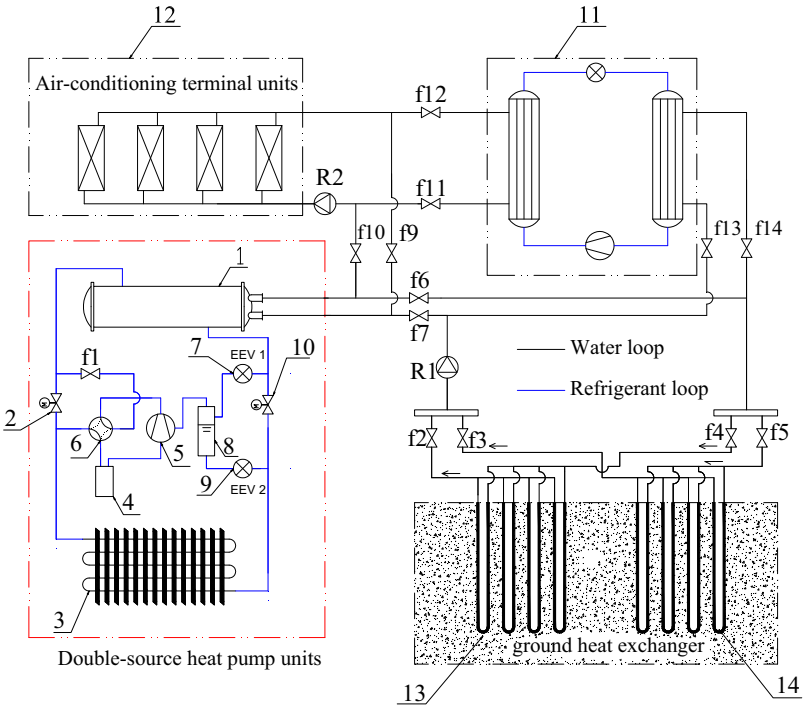

1-Condenser 2-Solenoid valve 3-Collector/evaporator 4-Gas-liquid separator 5-Compressor 6-Four-way reversing valve 7-A throttle valve 8-Economizer 9-Two-stage throttle valve 10-Solenoid valve 11-Ground source heat pump units 12-Air terminal device 13-Soil series heat storage heat exchanger 14-Cooling series of soil heat exchanger f1~f14-Switch valve R1~R2-Circulating pump

Fig. 1. Schematic diagram of MSHHPS for heating and air conditioning.

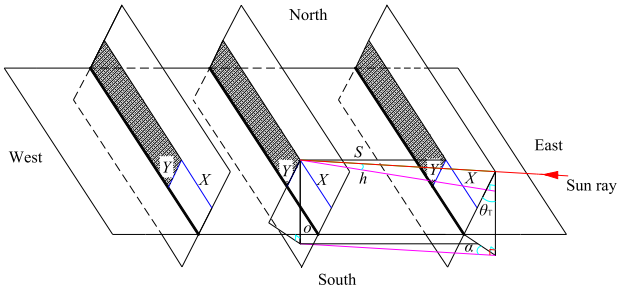

Fig. 2. Schematic diagram of fin blocked factor geometric relation.

intervals between the fins are small, there will be shielding before and after each fin so that the fins receive different solar heat radiation in different locations. The barrier factor is a parameter evaluating the fins' mutual barrier degree, defined as the ratio of the fin area that received solar radiation and the total area of the fin. The mathematical model of the barrier factor is established by the geometric relationship between the fin and fin projection. Schematic diagram of fin blocked factor geometric relations is showed in Fig. 2. Because the formula derivation process is complex, through geometric relations in Fig. 2 and the solar radiation correlation theory, the following formulas are obtained [20]:

$$X^2(1+\tan^2\theta_T) \pm 2X\frac{S\tanh\sin\theta_T}{\sin\alpha\cos^2\theta_T} + \frac{S^2\tan^2 h}{\sin^2\alpha\cos^2\theta_T} - \frac{S^2(1+\tan^2 h-\sin^2\alpha)}{\sin^2\alpha} = 0, \quad (\alpha<0, \text{“}-\text{”}; \alpha>0, \text{“}+\text{”}) \tag{1}$$

$$Y = H \pm \frac{S\tan h}{\sin\alpha\cos\theta_T} - \tan\theta_T X, \quad (\alpha<0, \text{“}+\text{”}; \alpha>0, \text{“}-\text{”}) \tag{2}$$

The occlusion of the fin at a given moment can be calculated by formulas (1), (2), and according to the barrier factor definition, the mathematical model of each factor can be calculated according to the fin occlusion type:

$$F = \frac{(L-X)(H-Y)+XH}{LH} \tag{3}$$

Selecting the partition of the lumped parameter method, this method in the separated type heat pipe mode based on the refrigerant state is divided into three zones: cooling zone, two-phase zone and overheated zone; in the vapor compression mode based on the refrigerant state it is divided into two zones: the two-phase zone and overheated zone, where the lumped parameter method is used in each area. We make the following assumptions: (1) The flow of refrigerant inside the pipe is axial one-dimensional homogeneous flow; (2) The resistance loss in the evaporator is ignored; (3) The gas phase and liquid phase are in a state of thermal equilibrium; (4) The effect of the pipe wall surface frost in low temperature conditions is ignored.

(1) The heat transfer equation of the energy balance flow on the side of the refrigerant is:

$$dQ_e = m_{r1}(h_{r4}-h_{r3}) \tag{4}$$

$$dQ_e = \alpha_{il}dA_i(T_{rm}-T_{tw}) \tag{5}$$

For the single-phase zone (superheat region, subcooled region), the refrigerant does not undergo a set state change, and the heat exchange coefficient can be calculated by the Dittus-Boelter heat transfer correlation:

$$\alpha'_{il} = \frac{\lambda_r \cdot Nu_i}{d_i} \tag{6}$$

For the two-phase regions, the heat exchange coefficient h_{i1} is calculated by the Shah [21] correlation:

$$\alpha''_{i1} = \alpha'_{i1}\left[(1-x)^{0.8} + \frac{3.8x^{0.76}(1-x)^{0.04}}{Pr^{0.38}}\right] \tag{7}$$

(2) The energy balance of the air side flow heat transfer equation:

$$dQ_{as} = \alpha_{as} dA_o (T_{am} - T_{tw}) \tag{8}$$

The collector/evaporator surface is coated with selective absorption coating such that it can absorb ambient air and absorb solar energy. To simplify the model, we will absorb the solar energy converted into the radiation convection heat transfer coefficient and add to the air-side convection heat transfer coefficient, this being the air-side heat transfer coefficient. The radiation heat exchange coefficient can be calculated by the following formula:

$$A'_3 = n_1\left(2HL_1 - \frac{\pi d_0^2}{4}\right)[(M+1)(N-1)+2] + \frac{1}{2}\pi d_0 n_1 (l - N\delta) + \frac{1}{4}\pi^2 d_0 (n_1 - 1)L_1 \tag{9}$$

$$\alpha_{ai} = \frac{A'_3 \varphi I}{A_3 \Delta t} \tag{10}$$

$$\alpha_{as} = \alpha_{aj} + \alpha_{ai} \tag{11}$$

3.2. Condenser

The condenser model is similar to the evaporator model. The flow and heat transfer of refrigerant in the condenser is a complex process. To simplify the calculation, making the following assumptions [22,23]: (1) The pressure drop in the condenser is ignored; (2) In the condenser, the mass flow of refrigerant is equal to the mass flow of refrigerant in the compressor; (3) In the condenser pipe, the fluid is in the axial direction of one-dimensional homogeneous flow; (4) The axial heat conduction in the pipe wall is ignored; (5) The gas phase and the liquid phase are in a state of thermal equilibrium.

(1) The energy balance of the refrigerant flow heat transfer equation:

$$dQ_c = m_r (h_{r1} - h_{r2}) \tag{12}$$

$$dQ_c = \alpha_c dA_i (T_{rm} - T_{tw}) \tag{13}$$

The refrigerant does not change phase in the single-phase zone (superheat region, subcooled region), while the heat exchange coefficient can also be calculated by the Dittus-Boelter heat exchange coefficient correlation. The condensation of refrigerant is film condensation in the two-phase zone. The heat exchange coefficient can be calculated by the following formula:

$$\alpha_c = c'\lambda\left(\frac{\rho^2 gr}{q \times d'_{i1} \times \mu}\right)^{\frac{1}{3}} \tag{14}$$

(2) The energy balance of the cooling water side flow heat transfer equation is

$$dQ_w = m_w (h_{w2} - h_{w1}) \tag{15}$$

$$dQ_w = \alpha_w dA_o (T_w - T_{tw}) \tag{16}$$

3.3. Compressor

The compressor is responsible for the main part of the energy consumption in the whole system, and its refrigerant mass flow and power consumption can be calculated by the following formulas [24]:

$$M_r = \frac{V_h \eta_v}{v_{ci}} \tag{17}$$

$$P = V_h \cdot \frac{\eta_v}{\eta_i} \cdot P_e \cdot \frac{k}{k-1}\left[\left(\frac{P_e}{P_c}\right)^{\frac{k-1}{k}} - 1\right] \tag{18}$$

3.4. Thermal expansion valve

The changing process of the refrigerant through the thermal expansion valve is regarded as isenthalpic throttling; the establishment of its steady state lumped parameter model is as follows:

$$h_{v1} = h_{v2} \tag{19}$$

$$M_v = c_{vf} A_v \sqrt{\rho_{vi} \Delta P_v} \tag{20}$$

3.5. Refrigerant charge

The refrigerant charge has a significant influence on the operational performance of the evaporative cooling combined air conditioner, and refrigerant mainly exists in the condenser, evaporator, and compressor cavity. Therefore, the total refrigerant charge M in the combined air conditioner can be obtained by the following formulas [25]:

$$M = (M_{tp} + M_{sp})_{eva} + (M_{tp} + M_{sp})_{con} + M_{com} \tag{21}$$

$$M_{sp} = \sum \rho A \Delta x \tag{22}$$

$$M_{tp} = \sum\left[\frac{\rho_g}{1 + \frac{1-x}{x}\cdot\frac{\rho_g}{\rho_f}} + \left(1 - \frac{1}{1 + \frac{1-x}{x}\cdot\frac{\rho_g}{\rho_f}}\right)\rho_f\right] A \Delta x \tag{23}$$

3.6. The soil heat exchanger

In order to facilitate the establishment of the mathematical model, the following assumptions are made: (1) The interaction between the soil heat exchangers is ignored, while the vertical U-tube heat exchanger is regarded as a vertical single tube. The equivalent diameter is $D_{eq} = \sqrt{2}D$; (2) The moisture transfer and heat transfer caused by groundwater seepage is ignored, and the soil heat exchanger and the heat transfer process of the soil are regarded as the pure conduction.

This section uses the two-dimensional cylindrical coordinate system, where the two-dimensional unsteady equation of the soil heat exchanger [26] is:

$$\rho_s c_{ps} \frac{\partial T_s(t,z,r)}{\partial t} = \frac{\partial}{\partial z}\left(\lambda_s \frac{\partial T_s(t,z,r)}{\partial z}\right) + \frac{1}{r}\frac{\partial}{\partial r}\left(r\lambda_s \frac{\partial T_s(t,z,r)}{\partial r}\right) \tag{24}$$

Boundary conditions:

$$-\lambda_s \frac{\partial T_s(t,z,r)}{\partial r}\bigg|_{r=\frac{D_{eq}}{2}, 0\leqslant z\leqslant l_0} = \frac{q_l(t,z)}{\pi D_{eq}} \tag{25}$$

$$-\lambda_s \frac{\partial T_s(t,z,r)}{\partial r}\bigg|_{r=0, l_0<z\leqslant z_0} = 0 \tag{26}$$

$$-\lambda_s \left.\frac{\partial T_s(t,z,r)}{\partial r}\right|_{r=r_0,0\leqslant z\leqslant z_0} = 0 \quad \text{internal tube} \tag{27}$$

$$T_s(t,z,r)|_{r=r_0,0\leqslant z\leqslant z_0} = T_{s0}(t,z) \quad \text{external tube} \tag{28}$$

$$-\lambda_s \left.\frac{\partial T_s(t,z,r)}{\partial z}\right|_{z=0,\frac{D_{eq}}{2}\leqslant r\leqslant r_0} = h_a[T_0 - T_s(t,0,r)] \tag{29}$$

The calculating formulas of q_1 and T_z are respectively:

$$q_1(z,t) = \frac{[T_{sf}(z,t) - T_{sr1}(z,t)]}{\frac{1}{\pi D_{eq} h_{sf}} + \frac{R_0}{\pi D_{eq}} + \frac{\ln(1+\Delta r/D_{eq})}{2\pi\lambda_s}} \tag{30}$$

$$T_z = T_a + \frac{a_s \cdot I_T}{h_a} \tag{31}$$

Initial conditions:

$$T_{s0}(t,z) = T_{sm} + T_{am} \cdot e^{-z\sqrt{\frac{\pi}{at_c}}} \cos\left(\frac{2\pi}{t_c}t - z\sqrt{\frac{\pi}{at_c}}\right) \tag{32}$$

The governing equations and boundary conditions of fluid within the tube of the heat exchangers are as follows:

(1) Governing equations

$$\frac{\partial T_{sf}(t,z)}{\partial t} + \upsilon_{sf}\frac{\partial T_{sf}(t,z)}{\partial z} = \frac{-\dot{4}q_l(t,z)}{\rho_{sf}c_{psf}\pi D_{eq}^2} \tag{33}$$

(2) Boundary conditions

$$\begin{aligned} &T_{sf}(t,0) = T_{co} \quad \text{Cooling condition} \\ &T_{sf}(t,0) = T_{eo} \quad \text{Heating condition} \end{aligned} \tag{34}$$

(3) Initial condition

$$T_{sf}(0,z) = T_{s0}(t_0,z) \tag{35}$$

3.7. The GSHP unit

The GSHP unit is a conventional water/water heat pump unit, whose performance is mainly affected by the evaporator and condenser side fluid temperature in constant flow conditions. To simplify the calculation, the performance of the GSHP unit have been derived from mathematical regression based on the performance

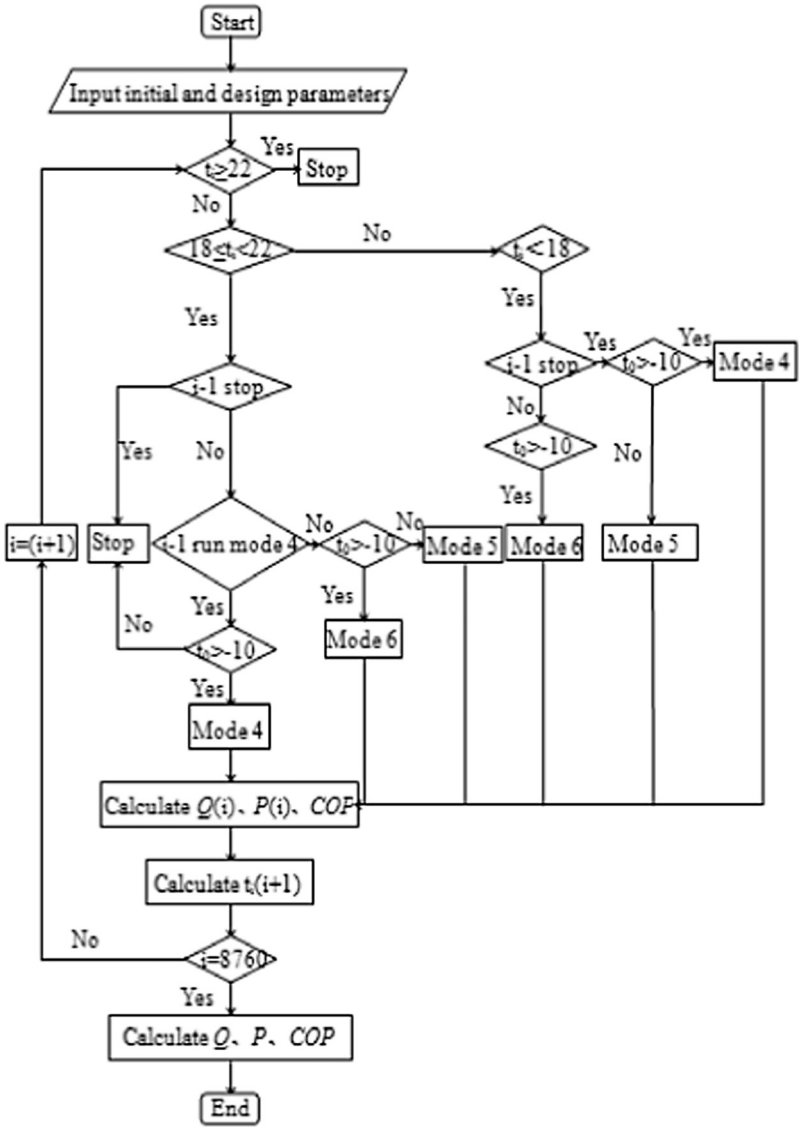

Fig. 3. Schematic diagram of MSHHPS simulation algorithm in heating period.

data under different test conditions provided by the product manufacturer:

$$Q_{hp} = a_1 T_{ei} + b_1 T_{ci} + c_1 \quad (36)$$

$$P_{hp} = a_2 T_{ei} + b_2 T_{ci} + c_2 \quad (37)$$

3.8. Simulation process of the MSHHPS

Fig. 3 is a flow chart of the MSHHPS simulation solution in the heating period, based on the upper and lower limits of outdoor temperature control. It can achieve three heating modes: when the ambient temperature is high, or the ambient temperature is low while the solar radiation is strong, Mode 4 has priority to run; when the outdoor temperature is lower and the solar radiation is weak, Mode 5 is operated; when Mode 4 can run efficiently but it difficult to meet the demand of the heating load, Mode 6 is operated.

Fig. 4 is a flow chart of the MSHHPS simulation solution in the cooling period, with two cooling modes. Mode 2 has priority to run because the soil temperature in the cold regions is low after the heating period. When Mode 2 cannot meet the demand of the cooling load, Mode 3 is operated.

Besides, considering that in the summer cooling is also needed, the buried tubes heat exchanger is divided into a cooling series and a heat storage series. When the ambient temperature is higher than the set temperature of the separate heat pipe for soil heat storage, Mode 1 is operated.

4. Operating characteristics analysis of MSHHPS in whole year

In a typical cold region, taking a 477 m^2 residential area of Harbin as the research object, building energy consumption simulation software DeST is used to calculate the building's annual hot and cold load, with the following results: In the heating period, the maximum heat load of the building heating is 92.80 kW, the accumulative total heat load is 283.40 GJ; in the cooling period, the maximum cooling load is 46.8 kW, the accumulative total cooling load is 70.10 GJ.

Based on the above model and object, the computer program for the whole annual running system dynamic simulation has been done. The simulation program includes three main stages: (1)

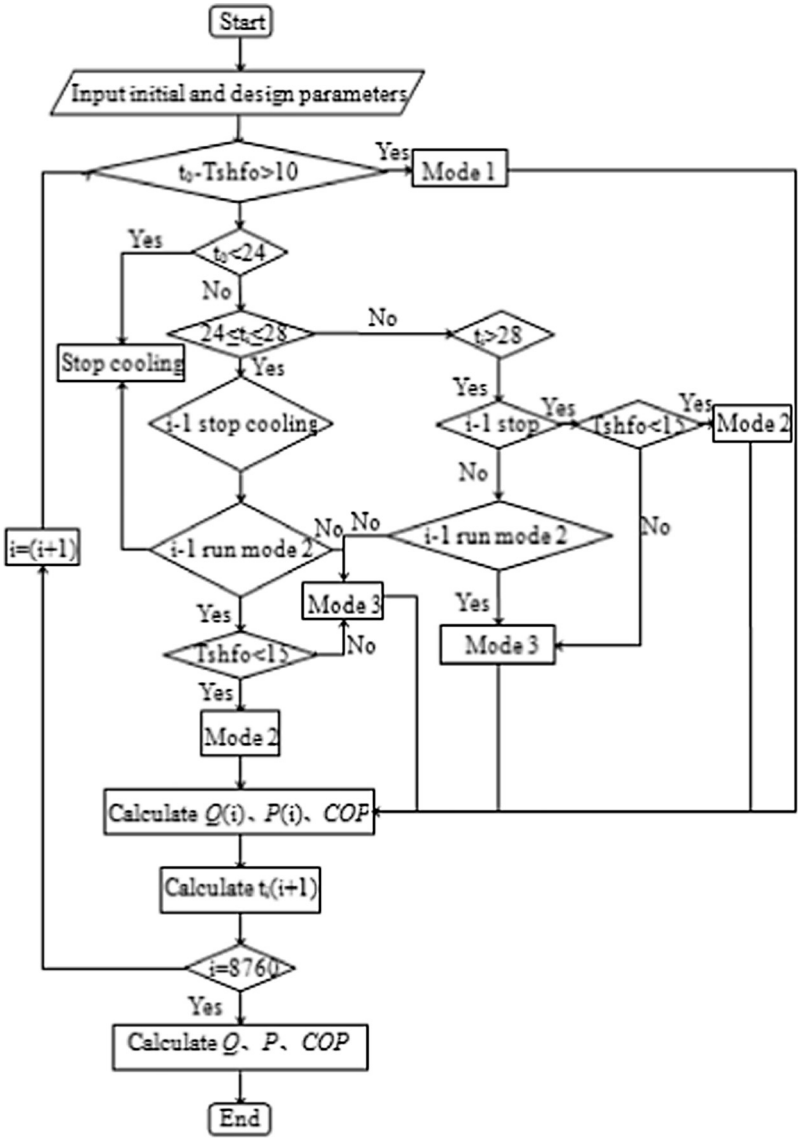

Fig. 4. Schematic diagram of MSHHPS simulation algorithm in cooling period.

The heating stage (October 15th–April 15th); (2) Heat storage, cooling stage (June 1st–August 31st); (3) Heat storage stage (April 16th–May 31st, September 1st–October 14th). The main parameters of the simulation are shown in Table 1.

Fig. 5 shows the change of the MSHHPS operating modes throughout the year. It can be seen that Mode 1 runs with an annual operation time of 1897 h in the non-heating period. Mode 2 runs individually at the beginning and end of the cooling period; Mode 2 and Mode 3 run intermittently in the middle of the cooling period, where the running time are 386 h and 285 h respectively. During the heating period, three kinds of heating modes run alternately. Mode 4 runs at the beginning and end of the heating period. With gradual decrease of the outdoor temperature, Mode 4 running separately cannot meet the heating demand, so the system runs Mode 6. In the middle of the heating period, the system mainly runs Mode 5. The running times of Mode 4, Mode 5 and Mode 6 are respectively 1039 h, 209 h, and 936 h.

Fig. 6 shows the daily change curve of heat storage in the soil for the cooling and heat storage series of buried tubes heat exchangers. As mentioned above, the heat stored by the heat storage series buried tube comes from the outdoor air and solar energy in the heating period. As can be clearly seen from the figure, the heat stored by the heat storage series in the non-heating period is increased gradually with an increase of the ambient temperature and solar radiation intensity. The heat stored by the cooling series buried tubes is mainly from the heat rejection of the summer air conditioning system. Under the influence of the air conditioning load, the heat storage of the cooling series buried tubes varies greatly. Due to the lower number of tubes in the cooling series of soil buried tube heat exchanger, the daily heat extraction in the heating period is less than that of the heat storage series.

Fig. 7 shows the change of the soil temperature field around the borehole heat exchanger at depths of 40 m in the ground for the heat storage series and the cooling series. It can be seen that the thermal balance of the soil can be ensured by every location of the soil temperature field around the buried tubes heat exchanger in the operating cycle. As the heat dissipation effect of the external tubes is better than that of the internal tubes, the annual soil temperature change around the internal buried pipe heat exchanger is larger than that of the external tubes. Due to the length limitation of the paper, the temperature field of the soil around the internal tubes is only analyzed. In the center of the buried tubes heat exchanger (r = 0.10 m), the highest temperature of the heat storage series internal tubes is 12.8 °C, the lowest temperature is 3.9 °C, and the magnitude of change is 8.9 °C; the highest temperature of the cooling series internal tube is 16.5 °C, the lowest temperature is 3.4 °C, and the magnitude of change is 13.1 °C. With greater distance from the center of the tube, the temperature change of the soil gradually decreases and tends to a fixed value.

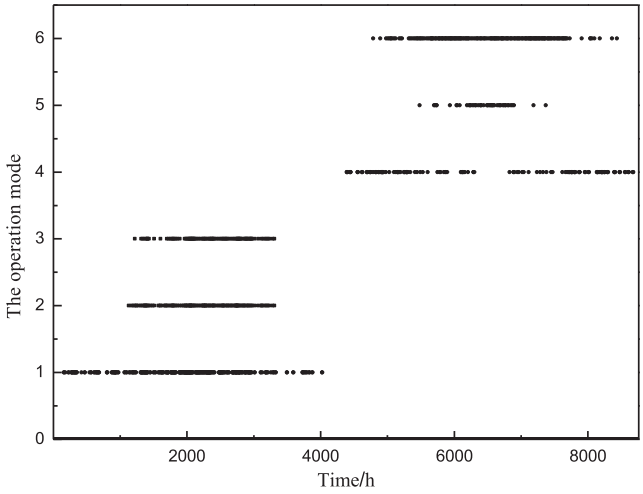

Fig. 5. The operation modes of the system in a typical year.

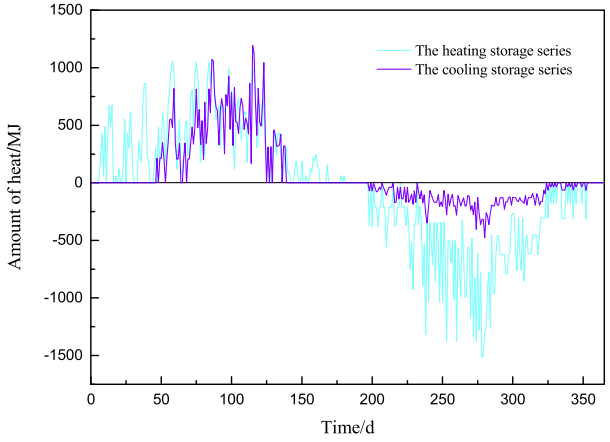

Fig. 6. Curves of daily total heat transferred from soil by different U-tube ground exchangers in a typical year.

Fig. 8 shows the annual running *COP* of the MSHHPS in each mode of operation. In the summer, it can be seen that the *COP* of the system changes greatly, with the maximum value of 23.21 and minimum value of 4.06, with the average value of 7.63. This

Table 1
Basic parameters of simulation.

Ground-source heat pump unit capacity Q_{HP}	62.5 kW	The depth of soil heat exchanger d_p	80 m
Air-source heat pump unit capacity Q_{HA}	37.2 kW	The density of ethylene glycol ρ_{sf}	1030 kg/m^3
Mode 2 temperature control parameter T_{sc}	15 °C	The specific heat of ethylene glycol c_{sf}	3831 J/(kg·K)
Time step$\Delta\tau$	3600 s	The density of air ρ_a	1.2 kg/m^3
Mode 4 close temperature T_{odl}	−18 °C	The specific heat of the air c_{pa}	1000 J/(kg·K)
Mode 1 start temperature difference d_{t0}	12 °C	The buried tubes diameter D	0.045 m
The air conditioning indoor design temperature T_{rcd}	26 °C	The density of the soil ρ_s	2120 kg/m^3
The heating indoor design temperature T_{rhd}	20 °C	The heat capacity of the soil c_{ps}	1975 J/(kg·K)
The soil temperature conductivity	1.89 W/(m·K)	Compressor volumetric efficiency η_v	0.6996
The permitted indoor temperature fluctuation dt	2 °C	Adiabatic coefficient κ	1.18
Inside and outside diameter of evaporator d_{eo}/d_{ei}	0.025/0.0235 m	Compressor indication efficiency η_i	0.78
Fitness factors of heat pump unit	a_1 = 0.5787	Inlet water temperature of indoor exchanger of heating mode T_{hd}	45 °C
	b_1 = 0.098		
	c_1 = 12.5305		
	a_2 = 0.0473	Heat exchange area of a single evaporator A	46.83 m^2
	b_2 = 0.0475		
	c_2 = 0.7758		
Inside and outside diameter of condenser d_{co}/d_{ci}	0.013/0.011 m	Radiation efficiency φ	0.95

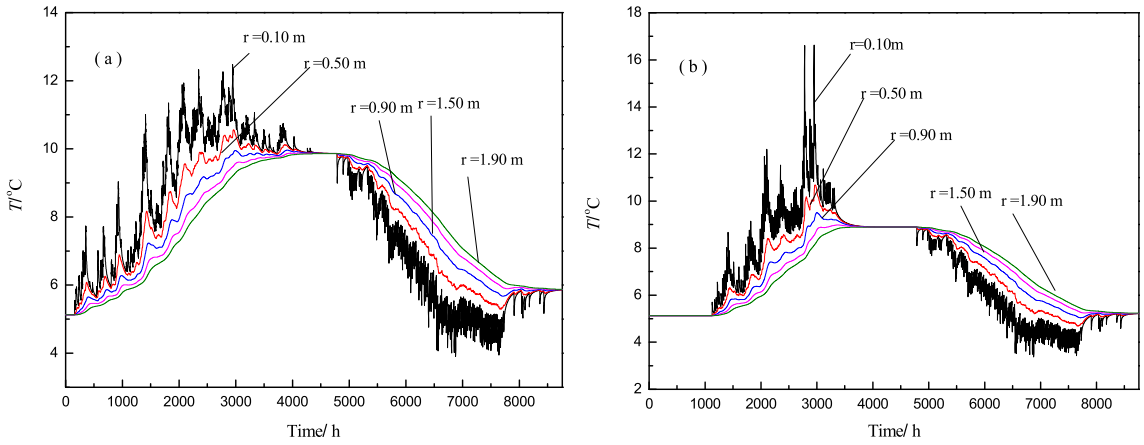

(a) The heat storage series internal tube (b) The cooling series internal tube

Fig. 7. Curves of the soil temperature field around soil heat exchangers.

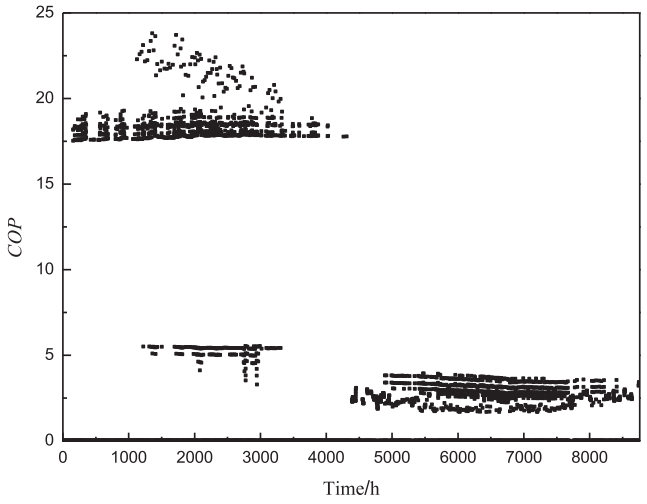

Fig. 8. The *COP* of system in the whole year.

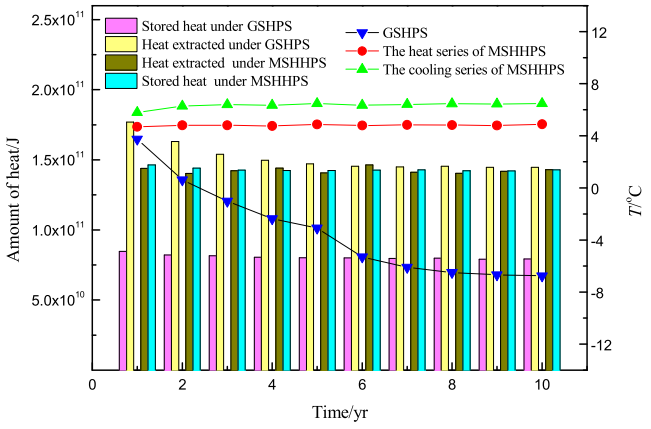

Fig. 9. The changes of heat stored/extracted and the soil temperature field in continuous operation for 10 years.

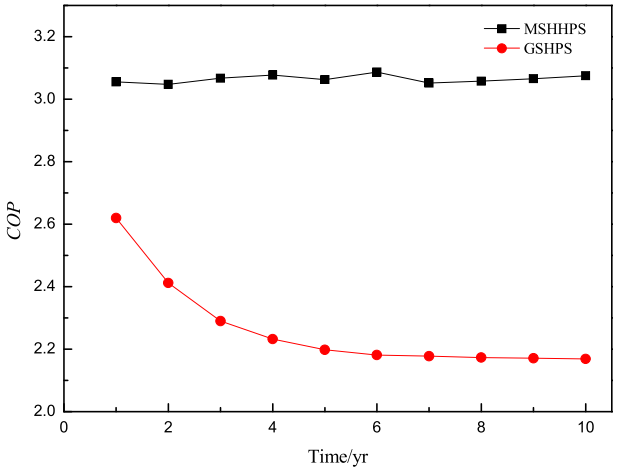

Fig. 10. The annual average *COP* of systems for 10 year.

is mainly because it consists of two cooling modes in the cooling period, the soil directly cooling mode does not require power consumption of the compressor, and only the circulating pump and fan coil work. In the winter, the variation of the *COP* value is low. The *COP* value is mainly concentrated at about 3, with the average value of 2.83. This is because the three heating modes are heat pump heating in the heating period. Mode 1 does not need the compressor to be started and can complete heat storage with the fan and circulating water pump, so the *COP* of Mode 1 is mainly concentrated around 18.0.

The soil heat transfer situation of GSHPS and MSHHPS running for 10 years is shown in Fig. 9. As can be seen from the figure, the heat extraction and injection of buried tube heat exchangers basically achieve a balance due to seasonal thermal storage function of the MSHHPS. After 10 years of continuous operation, the soil annual average temperatures around the cooling series and heat storage series buried tube heat exchangers rise by 0.68 °C and 0.18 °C, respectively. After 10 years of continuous operation for GSHPS, compared with the MSHHPS, the heat extraction of buried tube heat exchangers is basically same but the heat storage is far below the heat extraction. It causes the soil temperature around the buried tube heat exchangers to decrease year by year. The soil temperature around the buried tube heat exchangers of GSHPS declines by 9.08 °C.

The annual average *COP* of GSHPS and MSHHPS running for 10 years is shown in Fig. 10. As can be seen from the figure, the annual average *COP* of MSHHPS maintains at around 3.1. But for GSHPS, the annual average *COP* decreases year by year with the increase of the running time and tends to be stable eventually.

The annual average *COP* decreases from 2.62 to 2.16, which decreases by about 17.55%.

The annual operating parameters of GSHPS and MSHHPS running for 10 years in Harbin are given in Table 2. Compared with GSHPS, the average heating COP_h of the MSHHPS is increased by 49.21% and the average annual system *COP* is increased by 36%. Due to the long-term operation of GSHPS in the cold area, the soil temperature around the buried tube heat exchangers decreases year by year. Thus, the average cooling *COP* of GSHPS has increased by 27.78% compared with the MSHHPS. For the MSHHPS, the heat extraction and injection of the soil can basically achieve a balance under a year-round operation; the heat extraction is slightly less than the heat injection. The balance rate is 100.33% and the soil can achieve balance through its recovery. However, for GSHPS, the balance rate is 43.76%, which inevitably lead to soil thermal imbalance after long term operation. The cooling capacity of MSHHPS running for 10 years is 701.64 GJ, which the cooling capacity of mode 2 and mode 3 are 370.61 GJ and 331.03 GJ, respectively. The cooling COP_c of mode2 and mode3 are 20.37 and 4.19, respectively. The cooling capacity of GSHPS running for 10 years is 703.65 GJ. The heating capacity of MSHHPS running for 10 years is 2836.55 GJ, which the heating capacity of mode 4, mode 5 and mode 6 are 437.17 GJ, 662.88 GJ and 1736.60 GJ, respectively; The heating COP_h of mode3, mode4 and mode5 are 2.30, 2.94 and 2.93, respectively. The heating capacity of GSHPS running for 10 years is 2834.85 GJ. The total energy consumptions of the two systems are 1098.84 GJ and 1566.13 GJ respectively. After 10 years of continuous operation, compared with GSHPS, the MSHHPS can save electricity consumption 467.29 GJ and the energy-saving rate is 29.84%.

Table 2
Annual operating parameters of the MSHHPS and GSHPS system in Harbin.

Parameter	MSHHPS	GSHPS
Cooling capacity Q_c/GJ	701.64	703.65
Heating capacity Q_h/GJ	2836.65	2834.85
Power consumption *P*/GJ	1098.84	1566.13
Cooling COP_c	7.45	9.52
Heating COP_h	2.82	1.89
Comprehensive system *COP*	3.06	2.25
Soil balance rate ε	100.33%	43.67%
Energy saving/GJ	467.29	
Energy-saving rate/Θ	29.84%	

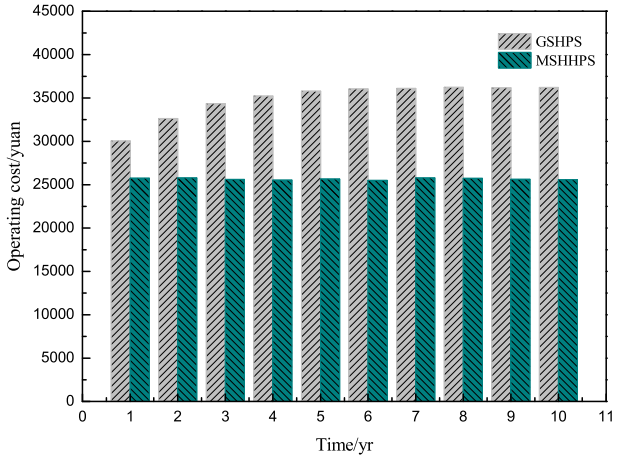

Fig. 11. The operating costs of both systems for 10 year.

The annual operating cost of the MSHHPS and the GSHPS is shown in Fig. 11. As can be seen from the figure, the operating costs of MSHHPS maintains at around 25,000 Yuan. But for GSHPS, The operating costs increases year by year with the increase of the running time and tends to be stable eventually. The saved operation costs increases from 4292 Yuan to 10,619 Yuan, which increases by about 147.71%.

Initial investment of the MSHHPS major equipment is shown in Table 3. Compared to the GSHPS, the MSHHPS just adds the double-source heat pump unit. This double-source heat pump unit merely changes the structure of the evaporator and the price is basically the same compared with 37 kW air source heat pump. The initial investment of double-source heat pump unit only account for 9.59% of GSHPS. The MSHHPS running for 10 years can save energy 467.29 GJ than GSHPS, about 129,800 kW h. If calculated by 0.8 Yuan/kW h, that is, it can save 103,800 Yuan. The static payback period of dual-source heat pump unit is 4 years and system revenue increases year by year with the growth of the running time.

Typical cold regions (Harbin, Urumqi, Changchun) are chosen as objects for simulation and calculation. Based on the soil thermal balance and the optimum start temperature difference of Mode

Table 3
Initial investment of major equipment [27].

Major equipment	Price	Initial investment/ ten thousand
Ground heat exchanger	80¥/m	23.04
Heat pump unit	84¥/m^2	4.01
Terminal device	60¥/m^2	2.86
Auxiliary equipment	21¥/m^2	0.95
Total investment		30.86
Double-source heat pump unit	800¥/kW	2.96

Table 4
Annual operating parameters of the MSHHPS in different regions.

Parameter	Mode	Harbin (E123°42′, N44°04′)	Changchun (E127°05′, N45°15′)	Urumqi (E87°36′, N43°45′)
Annual average temperature/°C		4.13	5.47	7.1
Minimum/Maximum outdoor temperature/°C		−28.7/32.8	−28.1/34.4	−25.0/38.8
Double-source heat pump unit close temperature/°C		−18	−18	−18
Separated type heat pipe start temperature difference/°C		12	18	19
Heating capacity Q_h/GJ	Mode 4	42.39	43.92	50.40
	Mode 5	39.83	32.02	12.85
	Mode 6	201.39	134.64	151.64
Total heating load/GJ		283.61	210.58	214.89
Cooling capacity Q_c/GJ	Mode 2	38.55	30.93	46.73
	Mode 3	31.88	46.28	31.79
Total cooling load/GJ		70.43	77.21	78.52
The soil balance rate ε		100.31%	100.62%	98.98%
The annual average *COP*		3.11	3.48	3.60
The system energy-saving rate Θ		29.45%	27.96%	27.88%

1, the system performance throughout the year is listed in Table 4. The simulation results showed that: the annual average *COP* were 3.11, 3.48, 3.60 and the soil balance rate reached 100.31%, 100.62%, 98.98% respectively. The energy-saving rate of the system were 29.45%, 27.96%, 27.88% respectively. It can be seen that the MSHHPS has good feasibility in different cold regions.

5. Conclusions

This paper proposed a MSHHPS in which solar energy, air energy and shallow soil heat energy can be comprehensively utilized and complemented, and the dynamic operating characteristics, energy efficiency and economy of the system were analyzed. The following conclusions can be drawn from this work:

(1) In the summer, the average COP_c value was 7.63. In the winter, the COP_h value was mainly concentrated at about 3, with the average value of 2.83. In the transition season, the heat storage COP_x was mainly concentrated around 18.
(2) Under the same condition, compared with the GSHPS, the average COP_h of the MSHHPS was increased by 49.21%, the average annual system *COP* was increased by 36%. In the initial investment, only a double-source heat pump unit was added in MSHHPS, accounting for 9.59% of initial investment and the static payback period was 4 years.
(3) Based on the simulation and calculation in Harbin, Urumqi and Changchun, the results showed that the MSHHPS has good feasibility in different cold regions.

Acknowledgement

The authors gratefully acknowledge the support from the Natural Science Foundation of China (grant no. 51406030).

References

[1] Tsinghua University Building Energy Conservation Center, Annual Report on China Building Energy Efficiency, China Architecture and Building Press, Beijing, 2014.
[2] M.F. Touchie, K.D. Pressnail, Testing and simulation of a low-temperature air-source heat pump operating in a thermal buffer zone, Energy Build. 75 (2014) 149–159.
[3] D.L.D. Silva, C. Hermes, C. Melo, Experimental study of frost accumulation on fan-supplied pipe-fin evaporators, Appl. Therm. Eng. 3 (2011) 1013–1020.
[4] X.M. Guo, Y.G. Chen, W.H. Wang, C.Z. Chen, Experimental study on frost growth and dynamic performance of air source heat pump system, Appl. Therm. Eng. 28 (2008) 2267–2278.
[5] J.C. Choi, J. Park, S.R. Lee, Numerical evaluation of the effects of groundwater flow on borehole heat exchanger arrays, Renew. Energy 52 (2013) 230–240.
[6] I. Sarbu, C. Sebarchievici, General review of ground-source heat pump systems for heating and cooling of buildings, Energy Build. 70 (2014) 441–454.
[7] S.H. Li, W.H. Yang, X.S. Zhang, et al., Soil temperature distribution around a U-tube heat exchanger in a multi-function ground source heat pump system, Appl. Therm. Eng. 29 (2009) 3679–3686.
[8] A. Capozza, M.D. Carli, A. Zarrella, Investigations on the influence of aquifers on the ground temperature in ground-source heat pump operation, Appl. Energy 107 (2013) 350–363.
[9] U. Desideri, N. Sorbi, L. Arcioni, D. Leonardi, Feasibility study and numerical simulation of a ground source heat pump plant, applied to a residential building, Appl. Therm. Eng. 31 (2011) 3500–3511.
[10] S.K. Chaturvedi, V.D. Gagrani, T.M. Abdel-Salam, Solar-assisted heat pump – a sustainable system for low-temperature water heating applications, Energy Convers. Manage. 77 (2014) 550–557.
[11] K. Bakirci, B. Yuksel, Experimental thermal performance of a solar source heat-pump system for residential heating in cold climate region, Appl. Therm. Eng. 31 (2011) 1508–1518.
[12] S.M.A. Rahman, R. Saidur, M.N.A. Hawlader, An economic optimization of evaporator and air collector area in a solar assisted heat pump drying system, J. Eur. Ceram. Soc. 76 (2013) 377–384.
[13] Y. Liu, J. Ma, G.H. Zhou, C. Zhang, W.L. Wan, Performance of a solar air composite heat source heat pump system, Renew. Energy 87 (2016) 1053–1058.
[14] C.H. Liang, X.S. Zhang, X.W. Li, X. Zhu, Study on the performance of a solar assisted air source heat pump system for building heating, Energy Build. 43 (2011) 2188–2196.
[15] K. Bakirci, O. Ozyurt, K. Comakli, O. Comakli, Energy analysis of a solar-ground source heat pump system with vertical closed-loop for heating applications, Energy 36 (2011) 3224–3232.
[16] V. Trillat-Berdal, B. Souyri, G. Fraisse, Experimental study of a ground-coupled heat pump combined with solar thermal collectors, Energy Build. 38 (2006) 1477–1484.
[17] A. Girard, E.J. Gago, T. Muneer, G. Caceres, Higher ground source heat pump *COP* in a residential building through the use of solar thermal collectors, Renew. Energy 80 (2015) 26–39.
[18] Q. Si, M. Okumiya, X.S. Zhang, Performance evaluation and optimization of a novel solar-ground source heat pump system, Energy Build. 70 (2014) 237–245.
[19] N. Pardo, A. Montero, J. Martos, J.F. Urchueguía, Optimization of hybrid-ground coupled and air source-heat pump systems in combination with thermal storage, Appl. Therm. Eng. 30 (2010) 1073–1077.
[20] X.B. Song, Research on the Optimization of Multi-source Heat Pump System in Severe Cold Area, Northeastern University, 2015.
[21] M.M. Shah, A general correlation for heat transfer during film condensation inside pipes, Int. J. Heat Mass Transfer 22 (1979) 547–556.
[22] Z.W. Han, Q.K. Liu, Y.Q. Zhang, et al., Feasibility study on novel room air conditioner with natural cooling capability, Appl. Therm. Eng. 108 (2016) 1310–1319.
[23] Y.X. Li, J.L. Yu, Theoretical analysis on optimal configurations of heat exchanger and compressor in a two-stage compression air source heat pump system, Appl. Therm. Eng. 96 (2016) 682–689.
[24] L.X. Zhao, C.L. Zhang, B. Gu, Neural-network-based polynomial correlation of single-and variable-speed compressor performance, HVAC&R Res. 15 (2009) 255–268.
[25] C.K. Rice, The effect of void fraction correlation and heat flux assumption on refrigerant charge inventory predictions, ASHRAE Trans. 93 (Part1) (1987) 341–367.
[26] Z.W. Han, M.Y. Zheng, et al., Numerical simulation of solar assisted ground source heat pump heating system with latent heat energy storage in severely cold, Appl. Therm. Eng. 28 (2008) 1427–1436.
[27] W. Xu, Handbook of Ground-Source Heat Pump Engineering, China Architecture and Building Press, Beijing, 2011.